Quantum theory of a two-photon micromaser

L. Davidovich,* J. M. Raimond, M. Brune, and S. Haroche†
Laboratoire de Spectroscopie Hertzienne de l'Ecole Normale Supérieure, 24, rue Lhomond, 75231 Paris Cedex 05, France
(Received 26 May 1987)

We present the quantum theory of a microscopic maser operating on a degenerate two-photon transition between levels of the same parity. We derive both a master equation and a Fokker-Planck equation for this system, and show that quantum effects may have a substantial influence on the behavior of the maser. They modify the oscillation threshold and make external triggering of this maser unnecessary, whereas, according to semiclassical theory, such a triggering is required to start up the maser oscillation. We derive the phase-diffusion properties of the field and show that the diffusion coefficient is complex in this case, its imaginary part being associated with a frequency shift of the field inside the cavity. We show that, in steady state, the photon-number statistics is sub-Poissonian for a wide range of pumping rates.

I. INTRODUCTION

Lasers operating on two-photon transitions between levels of the same parity have attracted considerable interest in the last 20 years.[1–9] This interest has been based on several grounds. These devices would present a faster growth of the field density than would usual lasers, and would be able to produce any frequency within the range allowed by the equation $\omega=\omega_1+\omega_2$, where $\hbar\omega$ is the energy difference between the two levels and ω_1,ω_2 are the frequencies of the two photons generated by the transition.[2] In addition, it has been pointed out that the field emitted by these devices might present interesting statistical properties, leading to the generation of "squeezed" states of light.[5,6]

In spite of this interest, however, no realization of a continuous-wave two-photon oscillator has been made so far. This is due to the exceedingly small gain on two-photon transitions between low-lying levels, and to the existence of very strong competing nonlinear processes (multiple-wave mixing and stimulated Raman effect). Only a few articles reporting two-photon stimulated emission and gain have been published so far.[10]

On the other hand, the development of Rydberg atom physics in the last few years, as well as of high-Q superconducting cavities, has led to the construction of masers which operate at a very low threshold, down to one atom at a time in the cavity.[11,12] Several aspects of these devices, which have been called "micromasers," have been studied recently.[13–15] In particular, they have been shown to offer the possibility of an unambiguous realization of a two-photon continuous-wave oscillator.[15]

In this article, we develop the quantum theory of a two-photon micromaser. We introduce new techniques, which allow a rigorous derivation of Fokker-Planck-like equations both for the diagonal and nondiagonal elements of the reduced density matrix of the field inside the cavity, in the photon-number representation. These techniques, although very simple and of general applicability in laser theory, do not seem to have been noticed before. They are based on a continuous approximation of the finite-difference master equation for the reduced density matrix of the field, and are therefore valid in principle only for large photon numbers. However, comparison of their solutions with the results obtained by numerical integration of the master equation shows that they remain valid even for small photon numbers.

The equations thus obtained allow a simple physical picture of the time-dependent behavior of the system, as well as of the steady-state solution. In particular, they demonstrate the existence of two time scales in the evolution of the photon-number distribution (similar results have been found in Ref. 13). The short-time scale corresponds to the evolution of the initial distribution towards a "local equilibrium" peak, often exhibiting sub-Poissonian statistics. The long-time scale corresponds to the slow diffusion of this peak, leading to the steady-state solution which, if the pumping rate is sufficiently high, may present extra peaks. These peaks are associated with a multistable behavior of the micromaser in the semiclassical limit.[15]

When applied to the off-diagonal matrix elements in the photon-number representation, the same techniques lead in a straightforward way to the phase-diffusion coefficient, which turns out to be complex for the two-photon micromaser. Its imaginary part corresponds to a frequency shift of the field inside the cavity, which can be interpreted as a self-induced frequency pulling, present even when the incoming atoms are resonant with the cavity frequency, and due to the quadratic Stark shift induced on the initial and final atomic levels by the field of the cavity, through the coupling with intermediate states (this shift is inexistent for a two-level model).

Even though these approximate equations are extremely useful for getting physical insight into the behavior of the system, we do not use them to get the numerical results concerning the statistics of the field. These results will be obtained directly from the master equation, since this equation is valid for any number of photons and, besides a numerical solution of the Fokker-Planck equation would involve its descretization anyway, leading thus again to a finite-difference equa-

tion. The numerical results thus obtained thoroughly confirm the physical analysis based on the approximate differential equations.

The system we are going to consider is the same as in Ref. 15: a two-photon maser operating on a degenerate two-photon transition such that there is a relay level $|i\rangle$ nearly halfway between the initial state $|e\rangle$ and the final state $|f\rangle$. The two-photon transition amplitude is thus greatly enhanced.

The atoms, initially prepared in the excited state $|e\rangle$, cross a cavity tuned to the frequency

$$\omega=(E_e-E_f)/2\hbar\ , \tag{1.1}$$

where E_e and E_f are the energies of the initial and final states, respectively. In this process, each atom undergoes a coherent second-order Rabi nutation[16,17] between the levels $|e\rangle$ and $|f\rangle$.

The practical feasibility of this device has been demonstrated in Ref. 15. The transition of interest occurs between $nS_{1/2}$ and $(n-1)S_{1/2}$ states, being thus two-photon allowed and one-photon forbidden. For alkali-metal Rydberg atoms, the intermediate level $(n-1)P_{3/2}$ has a detuning with respect to $(E_e+E_f)/2$ which is much smaller than E_e-E_f. In particular, it is exceedingly small for $n=40$ in rudibium and $n=44$ in cesium, but yet sufficiently large so as to allow one to discriminate the direct two-photon $nS_{1/2}\rightarrow(n-1)S_{1/2}$ process from the resonant one-photon cascade $nS_{1/2}\rightarrow(n-1)P_{3/2}\rightarrow(n-1)S_{1/2}$. The level configuration in this case is shown in Fig. 1. As shown in Ref. 15, a two-photon maser operating on a degenerate two-photon transition between these levels in a $Q\sim10^8$ cavity should oscillate with only about one atom at a time in the cavity and a few tens of microwave photons. Under these conditions, quantum effects may play an important role in the behavior of the system.

In Sec. II and in Appendix A, we derive the master equation for the two-photon micromaser, after reviewing some of the results of Ref. 15. The semiclassical evolution is analyzed in Sec. III, and the stability of the zero-intensity point is considered. Both the effect of thermal photons and the velocity spread of the atoms in the cavity are taken into account. In Sec. IV, we derive a Fokker-Planck equation for the photon-number distribution, and we discuss the steady-state solution and the approach to equilibrium. We show in particular that, even though the semiclassical theory predicts that, at low temperatures, an external field is necessary to start the laser oscillation[15] (even if one is above the oscillation threshold), quantum theory on the contrary predicts that, above threshold, the system will start oscillating by itself, without need of a triggering field. In Sec. V, we study the phase diffusion of the field inside the cavity, and establish the existence of a self-induced frequency pulling. The method used for this study is quite general, and is applied in Appendix B to the Scully-Lamb model[18] as well as to the one-photon micromaser. In Sec. VI, we show that, under certain conditions, the field inside the cavity exhibits a sub-Poissonian statistics. Fluctuation properties of the field are discussed in Appendix C. Our conclusions are summarized in Sec. VII.

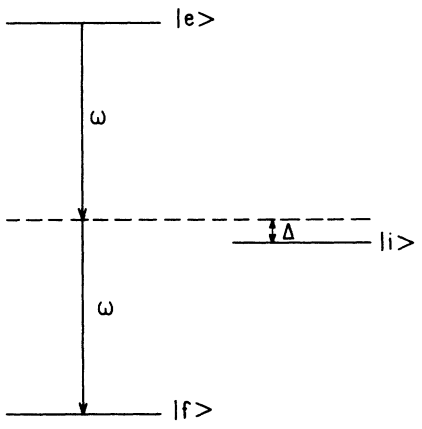

FIG. 1. Energy levels relevant to the two-photon micromaser.

II. THE MASTER EQUATION

The Hamiltonian corresponding to the system described in Sec. I can be written as[15]

$$H=H_{\rm at}+H_F+H_{\rm int}\ , \tag{2.1}$$

where $H_{\rm at}$, H_F, and $H_{\rm int}$ are, respectively, the atom, field, and interaction terms

$$H_{\rm at}=E_e\,|e\rangle\langle e|+E_i\,|i\rangle\langle i|+E_f\,|f\rangle\langle f|\ , \tag{2.2}$$

$$H_F=\hbar\omega(a^\dagger a+\tfrac{1}{2})\ , \tag{2.3}$$

$$H_{\rm int}=\hbar\Omega_{ei}(a\,|e\rangle\langle i|+a^\dagger|i\rangle\langle e|)+\hbar\Omega_{if}(a\,|i\rangle\langle f|+a^\dagger|f\rangle\langle i|)\ . \tag{2.4}$$

In these equations, a and $a^\dagger$ are the photon annihilation and creation operators, while Ω_{ei} and Ω_{if} are the elementary one-photon Rabi frequencies

$$\Omega_{ei}=-\langle e|D|i\rangle\mathcal{E}_0/\hbar\ , \tag{2.5}$$

$$\Omega_{if}=-\langle i|D|f\rangle\mathcal{E}_0/\hbar\ , \tag{2.6}$$

where $\langle e|D|i\rangle$ and $\langle i|D|f\rangle$ are the matrix elements of the electric dipole operator D and $\mathcal{E}_0$ is the field "per photon" in the cavity (of effective volume V)

$$\mathcal{E}_0=(\hbar\omega/2\epsilon_0V)^{1/2}\ . \tag{2.7}$$

In $H_{\rm int}$, one has made the rotating-wave approximation, which amounts to neglecting terms such as $a^\dagger|e\rangle\langle i|$ which couple levels whose energies differ by $E_e-E_i+\hbar\omega\simeq2\hbar\omega$. We also assume that the atom-field coupling is constant. This is generally not the case when the atoms move in an actual cavity mode. However, this variation can be taken into account by redefining $\mathcal{E}_0$.

The intermediate level $|i\rangle$ is detuned by the amount

$$\hbar\Delta=E_i-(E_e+E_f)/2 \tag{2.8}$$

from the average of the energies of the $|e\rangle$ and $|f\rangle$ states.

It has been shown in Refs. 15 and 17, using the dressed atom formalism, that the evolution of the system reduces to a two-level problem with an effective Rabi frequency of

$$\Omega(N)=\Omega_{ei}^2(2N+3)/\Delta \ , \tag{2.9}$$

where N is the number of photons in the cavity, so long as $|\Omega(N)/\Delta| \ll 1$ and $\Omega_{ei} \simeq \Omega_{if}$. These conditions are actually satisfied by the system described in Sec. I, and will be assumed throughout the paper. We may notice that $\Omega(0)$ does not vanish because of the two-photon spontaneous emission. If $|e,N\rangle$ and $|f,N+2\rangle$ represent the atomic states $|e\rangle$ and $|f\rangle$ with N and $N+2$ photons, respectively, in the cavity, and if $|e,N\rangle$ is the initial state of the system, we get then for the state of the system at time t

$$|e,N(t)\rangle = A(N,t)|e,N\rangle + B(N+2,t)|f,N+2\rangle \ , \tag{2.10}$$

where

$$A(N,t)=1+\frac{N+1}{2N+3}(e^{i\Omega(N)t}-1) \tag{2.11}$$

is the probability amplitude of finding the system in the initial state, and

$$B(N+2,t)=\frac{\sqrt{(N+2)(N+1)}}{2N+3}(e^{i\Omega(N)t}-1) \tag{2.12}$$

is the two-photon transition amplitude. Again, the fact that $A(0,t)\neq 1$ is due to spontaneous emission.

In order to write down the master equation corresponding to this system, we adopt the Scully and Lamb approach,[18] which is shown in Appendix A to be equivalent to the formulation in Ref. 13. In the interaction representation, the reduced density matrix for the field, $\rho(t)$, satisfies the equation of motion (under the conditions specified in Appendix A):

$$\dot{\rho}(t)=L\rho(t)+R[F(t_{\rm int})\rho(t)-\rho(t)] \ . \tag{2.13}$$

In this equation, $L\rho$ is associated with the loss mechanism

$$L\rho=\frac{\omega}{2Q}(N_T+1)(2a\rho a^\dagger - a^\dagger a\rho - \rho a^\dagger a) + \frac{\omega}{2Q}N_T(2a^\dagger \rho a - aa^\dagger \rho - \rho aa^\dagger) \ , \tag{2.14}$$

for a cavity with a quality factor Q and a thermal equilibrium mean-photon number given by N_T. The damping time of the cavity is $t_{\rm cav}=Q/\omega$.

The remaining term on the right-hand side of (2.13) stands for the atomic contribution to the reduced density operator of the field. The expression in square brackets is the variation of this operator due to the passage of a single atom through the cavity, during the interaction time $t_{\rm int}$, while $R=t_{\rm at}^{-1}$ is the atomic flux (average number of atoms arriving per unit time). As shown in Appendix A, writing Eq. (2.13) for the micromaser presupposes a Poissonian distribution for the arrival times of the incoming atoms in the cavity. The atomic contribution can be calculated in a well-known way[18] from Eq. (2.10) (we neglect atomic relaxation during $t_{\rm int}$):

$$\dot{\rho}_{NM}\,|_{\rm atom} = -R\rho_{NM}[1-A(N,t_{\rm int})A^*(M,t_{\rm int})] + R\rho_{N-2,M-2}B(N,t_{\rm int})B^*(M,t_{\rm int}) \ . \tag{2.15}$$

For $N=M$, the first term on the right-hand side represents the depletion of the N-photon state due to atomic transitions from $|e\rangle$ to $|f\rangle$; the second term on the right-hand side represents the contribution to ρ_{NN} from downward atomic transitions starting from the $(N-2)$-photon state.

Adding to (2.15) the contribution of the loss term, we obtain the full master equation in the interaction picture:

$$\dot{\rho}_{NM} = -R\rho_{NM}[1-A(N,t_{\rm int})A^*(M,t_{\rm int})] + R\rho_{N-2,M-2}B(N,t_{\rm int})B^*(M,t_{\rm int}) - \frac{\omega}{2Q}[N+M+2N_T(N+M+1)]\rho_{NM} + \frac{\omega}{Q}(N_T+1)\sqrt{(N+1)(M+1)}\rho_{N+1,M+1} + \frac{\omega}{Q}N_T\sqrt{NM}\,\rho_{N-1,M-1} \ , \tag{2.16}$$

which assumes a monoenergetic beam of atoms, since $t_{\rm int}$, which depends on the atomic speed, is fixed.

If one allows a velocity distribution for the atoms, the master equation in the interaction representation becomes

$$\dot{\rho}_{NM} = -R\rho_{NM}\left[1-\int_0^\infty dt_{\rm int}P(t_{\rm int})A(N,t_{\rm int})A^*(M,t_{\rm int})\right] + R\rho_{N-2,M-2}\int_0^\infty dt_{\rm int}P(t_{\rm int})B(N,t_{\rm int})B^*(M,t_{\rm int}) - \frac{\omega}{2Q}[N+M+2N_T(N+M+1)]\rho_{NM} + \frac{\omega}{Q}(N_T+1)\sqrt{(N+1)(M+1)}\rho_{N+1,M+1} + \frac{\omega}{Q}N_T\sqrt{NM}\,\rho_{N-1,M-1} \ , \tag{2.17}$$

where $P(t_{\rm int})$ is the interaction time distribution normalized so that

$$\int_0^\infty dt_{\rm int}P(t_{\rm int})=1 \ . \tag{2.18}$$

The master equation (2.17) is the central equation of this paper. From it we will get both the semiclassical behavior as well as the specifically quantum effects.

III. THE SEMICLASSICAL EVOLUTION

From (2.17), we can obtain an equation for the time rate of change of $\langle N\rangle$:

$$\langle \dot{N} \rangle = \sum_N N \dot{\rho}_{NN}$$
$$= 2R \left\langle \left[1 - \int_0^\infty dt_{\rm int} P(t_{\rm int}) \mid A(N, t_{\rm int}) \mid^2 \right] \right\rangle$$
$$- \frac{\omega}{Q} \langle N - N_T \rangle \ . \tag{3.1}$$

The first term on the right-hand side represents the contribution to $\langle \dot{N} \rangle$ from the downward transitions. The factor 2 comes from the fact that each transition yields two photons. The last term is associated with dissipation by the cavity, which makes $\langle N \rangle$ approach N_T within $t_{\rm cav}$. The semiclassical approximation is obtained by setting $N \gg 1$ and by assuming that the mean-square deviation of N is small, so that

$$\langle \mid A(N, t_{\rm int}) \mid^2 \rangle \simeq \mid A(\langle N \rangle, t_{\rm int}) \mid^2 \ . \tag{3.2}$$

In the limit $N \gg 1$, expressions (2.9), (2.11), and (2.12) can be simplified, so that

$$A(N,t) \simeq \exp(i \Omega_{ei}^2 N t / \Delta) \cos(\Omega_{ei}^2 N t / \Delta) \ . \tag{3.3}$$

This approximation amounts to neglecting the contribution of spontaneous emission terms.

We now define as in Ref. 13,

$$N_{\rm ex} = R t_{\rm cav} = t_{\rm cav} / t_{\rm at} \ , \tag{3.4}$$

$N_{\rm ex}$ being the number of atoms passing through the cavity during its damping time. We also introduce a reduced interaction time $\phi_{\rm int}$ and reduced photon numbers by

$$\phi_{\rm int} = 2 N_{\rm ex} \Omega_{ei}^2 t_{\rm int} / \Delta, \quad \bar{n} = \langle N \rangle / 2 N_{\rm ex}, \quad n_T = N_T / 2 N_{\rm ex} \ . \tag{3.5}$$

We get then, from (3.1) and (3.3),

$$\dot{\bar{n}} = - \frac{1}{t_{\rm cav}} \left[\bar{n} - n_T - \int_0^\infty d\phi_{\rm int} \tilde{P}(\phi_{\rm int}) \sin^2(\bar{n} \phi_{\rm int}) \right] , \tag{3.6}$$

where

$$\tilde{P}(\phi_{\rm int}) = \frac{\Delta}{2 N_{\rm ex} \Omega_{ei}^2} P \left[\frac{\Delta \phi_{\rm int}}{2 N_{\rm ex} \Omega_{ei}^2} \right] \tag{3.7}$$

is the atomic interaction time distribution expressed in terms of $\phi_{\rm int}$. Expressed as a function of the speed, this distribution should be Maxwellian. However, this is not the case for $\tilde{P}(\phi_{\rm int})$, since $\phi_{\rm int}$ is proportional to the inverse of the speed. Nevertheless, if this distribution is sufficiently peaked around some average value $\bar{\phi}_{\rm int}$, one can write approximately

$$\tilde{P}(\phi_{\rm int}) \simeq (2\pi\sigma)^{-1/2} \exp[-(\phi_{\rm int} - \bar{\phi}_{\rm int})^2 / 2\sigma^2] \ , \tag{3.8}$$

so that (3.6) can be replaced by an explicit expression,

$$\dot{\bar{n}} = - \frac{1}{t_{\rm cav}} \{ \bar{n} - n_T - \tfrac{1}{2} [1 - e^{-2\sigma^2 \bar{n}^2} \cos(2 \bar{n} \bar{\phi}_{\rm int})] \} \ . \tag{3.9}$$

This equation [or, alternatively, Eq. (3.6)] provides the semiclassical evolution of the number of photons in the cavity. It generalizes the corresponding equation in Ref. 15, since it includes both the effects of the velocity distribution and of thermal photons. The steady-state solutions are obtained from the equation

$$\bar{n} - n_T = \tfrac{1}{2} [1 - e^{-2\sigma^2 \bar{n}^2} \cos(2 \bar{n} \bar{\phi}_{\rm int})] \ . \tag{3.10}$$

This equation states simply that, in steady state, the losses, represented by the term on the left-hand side, equal the gain, expressed on the right-hand side. Both terms are represented on Fig. 2, as a function of $\bar{n}$, and for several values of $\bar{\phi}_{\rm int}$, n_T, and σ. The steady-state solutions are given by the intersections of the straight line with the gain curves. They are stable if the slope of

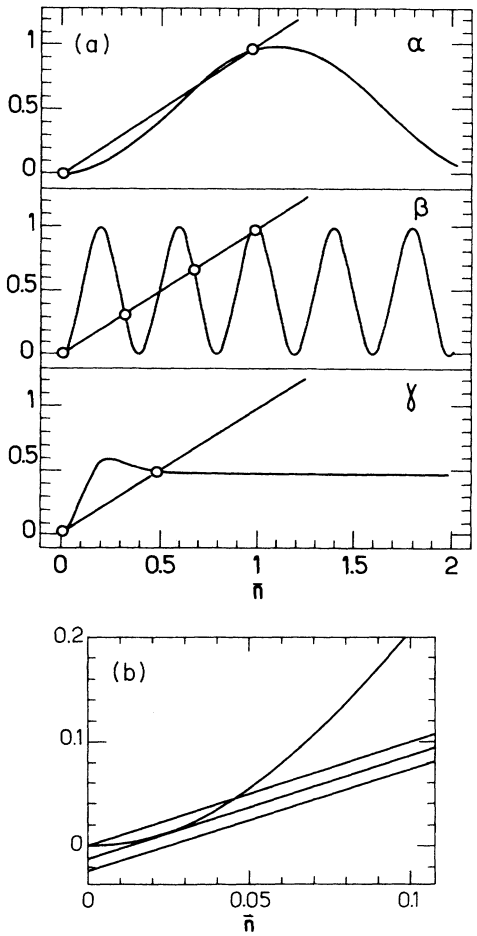

FIG. 2. Semiclassical model of the two-photon maser: loss and gain contributions to $\dot{\bar{n}}$ vs $\bar{n}$, where $\bar{n}$ is the normalized photon number $\langle N \rangle / 2N_{\rm ex}$. The loss term is linear in $\bar{n}$. (a) No thermal photons. The three curves correspond to (α) $\sigma = 0$, $\phi_{\rm int} = 0.9\pi/2$; ($\beta$) $\sigma = 0$, $\phi_{\rm int} = 5\pi/2$; (γ) $\sigma = \pi$, $\phi_{\rm int} = 3\pi/2$. Stable operation points are shown by circles. Note that $\bar{n} = 0$ is always a stable operation point. (α) is just above threshold. Disappearance of multistability as σ increases is apparent in curve (γ). (b) With thermal photons. $\phi_{\rm int} = 3\pi/2$. The three straight lines correspond, from top to bottom, to $n_T = 0$, 0.011, and 0.022, respectively. Triggering field is $n_T = 0.011$.

the absorption curve is larger than the slope of the gain curve at the intersection point. The threshold for oscillation is obtained when the straight line becomes tangent to the gain curve for the first time. For $n_T=0$ and $\sigma=0$, one recovers the solutions studied in Ref. 15, with their characteristic multistable behavior. In this case, the point $\bar{n}=0$ is always stable, even if one is above the threshold for oscillation (which occurs at $\phi_{\rm int}\simeq 0.9\pi/2$), implying that a triggering field is necessary to start the maser action. This feature, which is not present in the one-photon micromaser, was analyzed in detail in Ref. 15.

Changing n_T amounts to translating the straight line in Fig. 2 along a direction parallel to the vertical axis. We see that, as n_T increases, for a fixed value of $\phi_{\rm int}$, the stable points get displaced towards larger values, as expected. In particular, the stable point at the origin moves away from it, until it finally disappears, right after the straight line becomes tangent to the gain curve for the second time [see Fig. 2(b)]. This means that, above this critical value of n_T, the maser starts by itself due to the thermal photons, without need of any coherent triggering field. Alternatively, for a given n_T, there is a critical value of $\bar{\phi}_{\rm int}$ for which the maser starts by itself. These critical values can be calculated by considering the system of equations formed by Eq. (3.10) and the equation obtained by differentiating both sides of (3.10) with respect to $\bar{n}$, which, for $\sigma=0$, is written as

$$\phi_{\rm int}^{-1}=\sin(2\bar{n}\phi_{\rm int})\ . \tag{3.11}$$

In this way, we get, for instance, that the critical value of n_T is approximately 0.011 for $\phi_{\rm int}=3\pi/2$, yielding $N_T\simeq 0.7$ for $N_{\rm ex}=30$ (and $\sigma=0$). Of course, for such a low number of photons the semiclassical analysis may not be valid anymore, and we will see indeed in Sec. IV that it must be substantially modified when quantum effects are taken into account.

As $\sigma/\bar{\phi}_{\rm int}$ increases, the multistability disappears. For large values of this ratio, one cannot really use Eq. (3.8), which was based on the assumption that the velocity distribution is sufficiently sharp. However, going back to Eq. (3.6), we see that if $\tilde{P}(\phi_{\rm int})$ is very broad, one may replace the average over the squared sine by $\frac{1}{2}$, getting therefore as a unique stationary solution $\bar{n}=n_T+\frac{1}{2}$, which corresponds to an average number of photons given by

$$\langle N\rangle=N_{\rm ex}+N_T\ . \tag{3.12}$$

This limit leads to the usual laser theory: The average over speeds replaces the average over lifetimes present in the Scully-Lamb theory.[18] It could also be obtained directly from Eq. (3.9) by setting $\sigma\to\infty$.

The semiclassical picture discussed in this section does not take into account spontaneous emission effects. They will be considered in the following sections, where we will show that they may affect considerably the behavior of the system around $N=0$, specially for low $N_{\rm ex}$.

IV. FOKKER-PLANCK EQUATION: STEADY STATE, MULTISTABILITY, AND APPROACH TO EQUILIBRIUM FOR THE FIELD DIAGONAL MATRIX ELEMENTS

A. Recurrence relation for the steady state

From (2.17), we can see that the diagonal matrix elements in steady state satisfy the recurrence relation,

$$-R\rho_{NN}\left[1-\int_0^\infty t_{\rm int}P(t_{\rm int})\,|\,A(N,t_{\rm int})\,|^2\right]+R\rho_{N-2,N-2}\int_0^\infty dt_{\rm int}P(t_{\rm int})\,|\,B(N,t_{\rm int})\,|^2$$
$$-\frac{\omega}{Q}[N+N_T(2N+1)]\rho_{NN}+\frac{\omega}{Q}(N_T+1)(N+1)\rho_{N+1,N+1}+\frac{\omega}{Q}N_TN\rho_{N-1,N-1}=0\ , \tag{4.1}$$

with the definition

$$\rho_{-1,-1}=\rho_{-2,-2}=0\ . \tag{4.2}$$

As opposed to the one-photon case,[13,14] this recurrence relation does not admit any simple analytic solutions; due to the presence of the term $\rho_{N-2,N-2}$, it cannot be solved by the usual detailed balance argument.[18] We will therefore seek a continuous approximation of the discrete master equation (2.17), which will allow us to find an approximate steady-state solution. This solution will be useful to get physical insight into the behavior of the system. It will be shown to coincide very closely with the numerical solution of (4.1) and (4.2), so long as $N\gg 1$. Furthermore, the same approximation method, when applied to the equation for the off-diagonal matrix elements, will be useful to study the phase-diffusion properties of the field. However, the dynamical evolution of the system will be obtained numerically directly from (2.17). The master equation will also be required to study the behavior of the steady state close to $N=0$. This will be done in Sec. IV E, directly from (4.1) and (4.2).

B. Derivation of the Fokker-Planck equation

Let us define

$$n=N/2N_{\rm ex},\quad \delta=1/2N_{\rm ex}\ . \tag{4.3}$$

Let

$$\tilde{A}(n,\phi_{\rm int})=A(N,t_{\rm int})\ , \tag{4.4}$$

with N and $t_{\rm int}$ expressed in terms of n and $\phi_{\rm int}$ by (4.3)

and (3.5), so that, from (2.11),

$$|\tilde{A}(n,\phi_{\rm int})|^2=1-\frac{4(n+\delta)(n+2\delta)}{(2n+3\delta)^2}\times\sin^2\left[\frac{2n+3\delta}{2}\phi_{\rm int}\right] . \tag{4.5}$$

We also define a dimensionless time

$$\tau=Rt \tag{4.6}$$

and replace the discrete distribution $\rho_{NN}(t)$ by the continuous function

$$\rho(n,\tau)=\rho_{NN}(t) . \tag{4.7}$$

We get then from (2.17)

$$\frac{\partial}{\partial\tau}\rho(n,\tau)=-\rho(n,\tau)\left[1-\int_0^\infty d\phi_{\rm int}\tilde{P}(\phi_{\rm int})|\tilde{A}(n,\phi_{\rm int})|^2\right]+\rho(n-2\delta,\tau)\left[1-\int_0^\infty d\phi_{\rm int}\tilde{P}(\phi_{\rm int})|\tilde{A}(n-2\delta,\phi_{\rm int})|^2\right]$$
$$-2[n+N_T(2n+\delta)]\rho(n,\tau)+2(N_T+1)(n+\delta)\rho(n+\delta,\tau)+2N_T n\rho(n-\delta,\tau) . \tag{4.8}$$

We now expand this equation into powers of δ, keeping terms up to $O(\delta^2)$. This approximation is valid as long as $n\gg\delta$, that is, $N\gg1$, and $\delta\ll1$, that is, $2N_{\rm ex}\gg1$. We get then

$$\frac{\partial}{\partial\tau}\rho(n,\tau)=-\delta\frac{\partial}{\partial n}[a_1(n)\rho(n,\tau)]+\frac{\delta^2}{2}\frac{\partial^2}{\partial n^2}[a_2(n)\rho(n,\tau)]+O(\delta^3) , \tag{4.9}$$

where

$$a_1(n)=2\left[\int_0^\infty d\phi_{\rm int}\tilde{P}(\phi_{\rm int})\left[\sin^2(n\phi_{\rm int})+\frac{3\delta\phi_{\rm int}}{2}\sin(2n\phi_{\rm int})\right]-n+n_T\right] , \tag{4.10}$$

$$a_2(n)=4\int_0^\infty d\phi_{\rm int}\tilde{P}(\phi_{\rm int})\sin^2(n\phi_{\rm int})+2n(1+2N_T) , \tag{4.11}$$

and, according to (3.5) and (4.3), $n_T=\delta N_T$.

This is an equation of the Fokker-Planck type. It is easy to show that the same procedure, applied to the one-photon micromaser, leads precisely, except for the terms of $O(\delta)$ in (4.10), to the Fokker-Planck equation obtained in Ref. 13 by another method, which is valid in principle only for small times. The present approach is explicitly valid for all times. Besides, it allows, as we will show in Sec. V, the analysis of the behavior of the off-diagonal elements of the density matrix and therefore of the phase diffusion properties of the micromaser.

The first term on the right-hand side of (4.9) is the drift term; the second-order contribution is the diffusion term. One should notice that $a_2(n)\geq0$, yielding a positive-definite diffusion coefficient, as it should be. It is easy to show from (4.9) that

$$\frac{d}{d\tau}\langle n\rangle=\int_0^\infty n\frac{\partial\rho(n,\tau)}{\partial\tau}dn=\delta\langle a_1(n)\rangle , \tag{4.12}$$

which is just the semiclassical evolution equation (3.6), with the approximation $\langle a_1(n)\rangle=a_1(\langle n\rangle)$ and the omission of corrections of order δ. It is tempting to associate with $a_1(n)$ a potential defined by

$$U(n)=-\delta\int_0^n a_1(n')dn' , \tag{4.13}$$

which would govern not only the semiclassical evolution [Eq. (4.12) being thus analogous to that of a forced overdamped oscillator] but also the probability distribution. We will see, however, in the following that this last statement is not true, due to the n dependence of the diffusion coefficient.

C. Steady state

The steady-state solution of (4.9) is easily obtained:

$$\rho^S(n)=\frac{C}{a_2(n)}\exp\left[\frac{2}{\delta}\int_0^n\frac{a_1(n')}{a_2(n')}dn'\right] , \tag{4.14}$$

where C is a normalization constant. This expression diverges when $n\to0$, which is a consequence of the nonvalidity of (4.9) in this limit. It has the form of a Boltzmann distribution,

$$\rho^S(n)=\exp[-2V_F(n)/\delta] , \tag{4.15}$$

with an effective potential,

$$V_F(n)=-\int_0^n\frac{a_1(n')}{a_2(n')}dn'+\frac{\delta}{2}\ln a_2(n)-\frac{\delta}{2}\ln C . \tag{4.16}$$

This potential completely determines the behavior of $\rho^S(n)$, which is peaked around the absolute minimum of $V_F(n)$. If differs, however, from the semiclassical potential (4.13), precisely because of the n dependence of the diffusion coefficient. Since $\delta\ll1$, the second term on the right-hand side of (4.16) will give a small contribution, the same being valid for the δ-dependent term in $a_1(n)$. Thus, the extrema of $V_F(n)$ will practically coincide with the zeros of $a_1(n)$, which correspond to the steady-state operating points in the semiclassical model [unstable ones corresponding to the maxima of $V_F(n)$, stable ones to the minima].

We display in Fig. 3 the effective potential $V_F(n)$, for several values of $\phi_{\rm int}$, when σ and n_T are set equal to zero, and $N_{\rm ex}=30$. In the same figure, we show the potential obtained, through Eq. (4.15), from the numerical

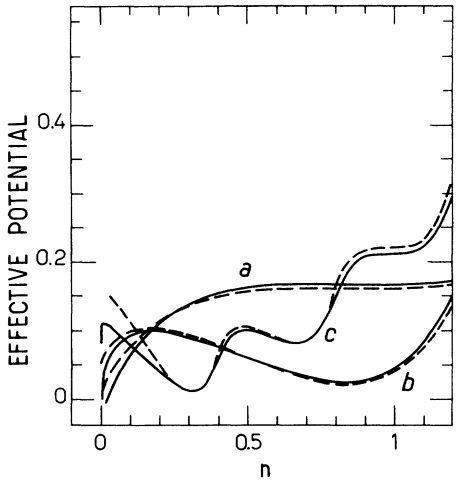

FIG. 3. Effective potential $V_F(n)$ and $V_M(n)$ for a, $\phi_{\rm int}=0.9\pi/2$; b, $\phi_{\rm int}=1.5\pi/2$; c, $\phi_{\rm int}=5\pi/2$. The solid curve corresponds to the potential V_F obtained from the Fokker-Planck equation; the dashed curve to V_M, obtained from the master equation. $\sigma=0$ and $n_T=0$.

solution of (4.1) and (4.2). We call this potential $V_M(n)$. The coincidence is remarkable, except for very small n, as expected. In Fig. 4, we show the potential $V_F(n)$ for $\bar{\phi}_{\rm int}=5\pi/2$ and several values of σ, still for $n_T=0$. The multistable nature of the solution disappears as σ increases. The limit $\sigma\to\infty$ is easily obtained from (4.10), (4.11), and (4.14). We get

$$\rho^S(n)\simeq C'(1+nl)^{(2+l)/\delta l^2}\exp(-2n/\delta l)\ , \tag{4.17}$$

where $C'=C/2$ and

$$l=1+2N_T\ . \tag{4.18}$$

This distribution has only one maximum, at $n\simeq\frac{1}{2}$, corresponding to

$$N\simeq N_{\rm ex}\ . \tag{4.19}$$

The disagreement with (3.12) is due to the N_T dependence of the diffusion coefficient, leading to an uncertainty in the number of photons which is bigger than the difference between (3.12) and (4.19).

For $l=1(N_T=0)$, one finds for the photon-number distribution,

$$P(N)\simeq\left[1+\frac{N}{2N_{\rm ex}}\right]^{6N_{\rm ex}}\exp(-2N)\ . \tag{4.20}$$

The semiclassical model threshold corresponds to the $\phi_{\rm int}$ for which the potential develops for the first time an extra minimum, besides the one around the origin. For $\sigma=0$ and $n_T=0$, we know already that the threshold is obtained for $\phi_{\rm int}\simeq0.9\pi/2$, and we see indeed that for this value of $\phi_{\rm int}$ there appears a minimum of $V_F(n)$ [and also of $V_M(n)$] around $n=1$. However, in this situation, $\rho^S(n)$ is still maximal for $n=0$, and the steady-state mean photon number is close to zero, as can be explicitly seen in Fig. 5, which exhibits $\langle N\rangle$ as a function of $\phi_{\rm int}$ for the steady state. The threshold condition is thus not the same as in the semiclassical model; a minimum of $V_F(n)$ for $n\neq0$ must exist, but its value must be lower than the value of $n=0$ (that happens for $\phi_{\rm int}\geq1.4\pi/2$; the corresponding threshold value of $\langle N\rangle$ is ~50, for $N_{\rm ex}=30$).

As $\phi_{\rm int}\to\infty$, the average photon number goes to a limit which is approximately given by (4.19). This is a consequence of the fact that, as $\phi_{\rm int}\to\infty$, the trigonometric functions in (4.10) and (4.11) oscillate very fast as n varies, and therefore can be replaced by their averages in the calculation of $\langle N\rangle$, which is precisely the effect produced by the limit $\sigma\to\infty$. It is not surprising, therefore, that the two limits yield the same value for $\langle N\rangle$.

In Fig. 6, we display the potential $V_M(n)$, obtained directly from (4.1) and (4.2), for $\sigma=0$, $\phi_{\rm int}=3\pi/2$, and different values of N_T (again $N_{\rm ex}=30$). Contrary to the semiclassical analysis, $V_M(n)$ has a minimum at $n=0$, independently of the value of N_T. This will be discussed in Sec. IV E. As N_T increases, the potential well around $N=30$ gets wider and flatter, because the diffusion coefficient $a_2(n)$ increases with N_T.

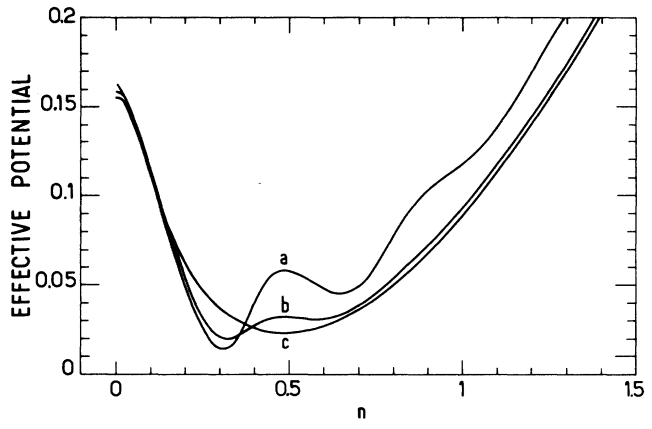

FIG. 4. Effective potential $V_M(n)$ for $\bar{\phi}_{\rm int}=5\pi/2$ and a, $\sigma=\pi/4$; b, $\sigma=\pi/2$; c, $\sigma=3\pi/2$.

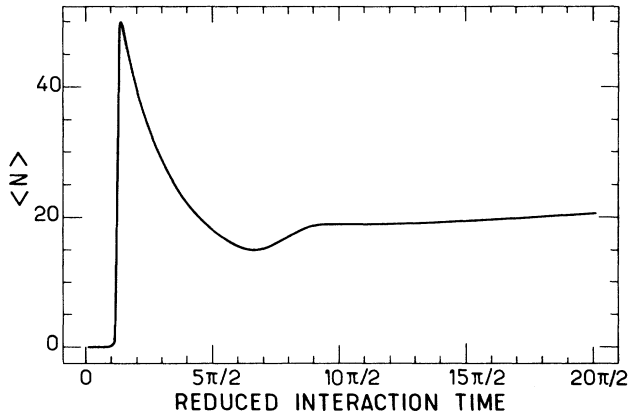

FIG. 5. Average photon number $\langle N\rangle$ in steady state, as a function of the reduced interaction time $\phi_{\rm int}$ ($\sigma=0$, $N_T=0$, $N_{\rm ex}=30$).

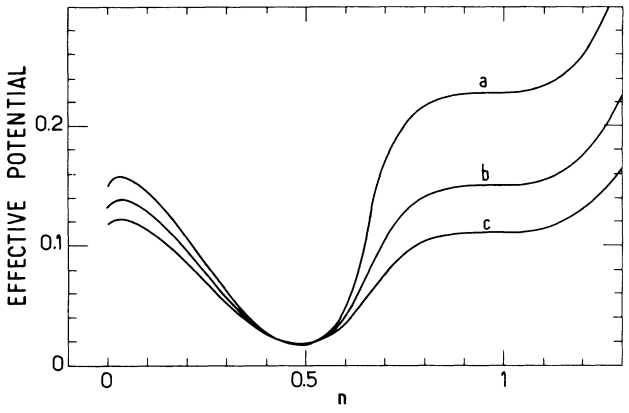

FIG. 6. Effective potential $V_M(n)$ for $\sigma=0$, $\phi_{\rm int}=3\pi/2$, $N_{\rm ex}=30$, and a, $N_T=0$; b, $N_T=0.3$; c, $N_T=0.7$.

Another distinction between the semiclassical analysis and the present treatment is that, in the former case, the steady-state solution depends on the initial condition (for instance on the presence of a triggering field). This is certainly not the case here; $\rho^S(n)$ is the same no matter what the initial condition is. The connection between these two results will be clarified in the following.

D. Local and global approaches to equilibrium

The Fokker-Planck equation (4.9) allows a simple physical picture of the time-dependent behavior of the statistics of the field.

Let us consider the time evolution of the system when $\rho(n)$ is initially peaked around an arbitrary n_0 value. The approach to equilibrium will proceed in general in two steps, corresponding to two quite different time scales.[19] Because of the drag term $a_1(n)$ in (4.9), the mean photon number will reach in a short time a value close to the nearest local minimum of $V_F(n)$ (as we will show below, the time scale of this process turns out to be $t_{\rm cav}$). Correspondingly, the initial peak will be displaced and, at the same time, its shape will change, turning into a "local equilibrium" distribution, often sub-Poissonian. Generally, this minimum is not the lowest one, and the state reached is only metastable. Because of the fluctuations [associated with the term $a_2(n)$], $\rho(n)$ will escape from this potential well and reach a more stable one. The corresponding passage times are usually much larger than $t_{\rm cav}$, and become infinite when $N_{\rm ex}\to\infty$; we recover, then, the semiclassical results. The solution will, in this situation, depend on the initial condition even for very large times since passage to other wells just does not occur, in this limiting case.

The local equilibrium behavior is obtained by setting, in (4.9), $a_2(n)$ equal to its value at the closest local minimum n_L of $V_F(n)$, and by expanding $a_1(n)$ around n_L, up to first order $n-n_L$. We get then for $\rho(n)$ the following equation:

$$\frac{\partial}{\partial\tau}\rho(n,\tau)=-\delta\frac{\partial}{\partial n}[a_1'(n_L)(n-n_L)\rho(n,\tau)]+\frac{\delta^2}{2}a_2(n_L)\frac{\partial^2}{\partial n^2}\rho(n,\tau)\ . \tag{4.21}$$

This equation is associated with a Ornstein-Uhlenbeck process.[19] Its solution, subject to the initial condition $\rho(n,\tau=0)=\delta(n-n_0)$, can be explicitly found and predicts an approach to equilibrium with a time constant $[\delta\,|\,a_1'(n_L)\,|\,]^{-1}$. Since $|\,a_1'(n_L)\,|$ is of order unity and in (4.21) time is measured in units of $t_{\rm at}$, this means that the time constant for the approach to local equilibrium is of the order of $N_{\rm ex}t_{\rm at}=t_{\rm cav}$. Of course, Eq. (4.21) is valid only if this local equilibrium time is much smaller than the passage time, since writing (4.21) is equivalent to assuming that initially $\rho(n)$ "sees" but the local

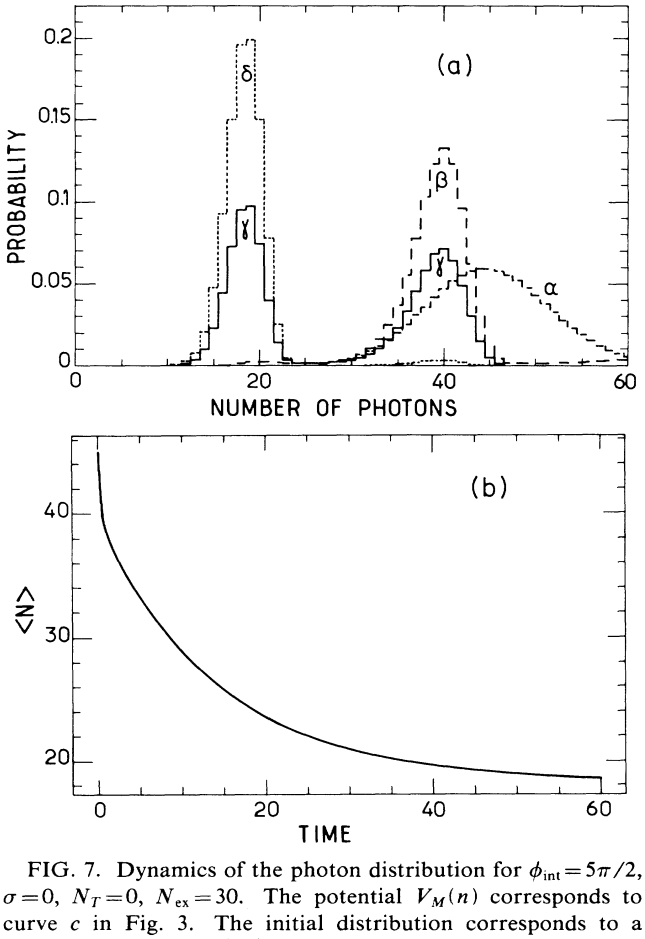

FIG. 7. Dynamics of the photon distribution for $\phi_{\rm int}=5\pi/2$, $\sigma=0$, $N_T=0$, $N_{\rm ex}=30$. The potential $V_M(n)$ corresponds to curve c in Fig. 3. The initial distribution corresponds to a coherent state with $\langle N\rangle=45$. (a) Evolution of the photon-number distribution: (α) $t=0$; (β) $t=0.5t_{\rm cav}$, (γ) $t=10t_{\rm cav}$; (δ) $t=60t_{\rm cav}$. Notice the very fast change from the initial coherent distribution to a sub-Poissonian one centered around the local minimum of $V_M(n)$ at $n=\frac{2}{3}$, corresponding to $N=40$. (b) Evolution of $\langle N\rangle$. Time is expressed in units of $t_{\rm cav}$. Note the change in slope around time $t\sim t_{\rm cav}$, corresponding to the transition from the fast drift to the local minimum to the slow passage to the absolute minimum.

minimum of $V_F(n)$.

On the other hand, the passage time, which governs the leaking of probability from one potential well into its neighbor, is given by Kramers's formula, which yields in the present case, in real time units[13,19]

$$T_p \simeq 2\pi t_{\rm cav} \left[|a_1'(n_L)|\, a_1'(n_1) \frac{a_2(n_1)}{a_2(n_L)} \right]^{-1/2} \times \exp\left[\frac{2}{\delta} [V_F(n_1) - V_F(n_L)] \right], \quad (4.22)$$

where n_1 is the value of n corresponding to the maximum of the potential between n_L and its neighbor. In other words, $V_F(n_1) - V_F(n_L)$ is the height of the potential barrier which separates the well around n_L from its neighbor.

From Eq. (4.22) and Fig. 3, we see that T_p is of the order of $t_{\rm cav}\exp(\alpha N_{\rm ex})$, where α is a constant of order 0.1. A similar analysis was applied in Ref. 13 to the one-photon micromaser, where the same kind of result is obtained. In particular, it is clear that when $N_{\rm ex} \to \infty$, so does the passage time, and the semiclassical limit is attained.

In Fig. 7(a), we display the time-dependent behavior of $\rho(n,\tau)$, starting from an initial coherent state,[20] for $\phi_{\rm int} = 5\pi/2$ and $N_{\rm ex} = 30$ (σ and n_T are set equal to zero). In this case, if one starts around the rightmost well of $V_F(n)$, depicted in Fig. 3(c), the passage time will be of the order of $20 t_{\rm cav}$. The local equilibrium distribution corresponds to the curve β in Fig. 7(a), which clearly exhibits a sub-Poissonian statistics. The evolution of the average number of photons is shown in Fig. 7(b). The exponential dependence of the passage time on $N_{\rm ex}$ is verified in Fig. 8 [the δ dependence of $V_F(n)$ is negligible for the values of $N_{\rm ex}$ considered in this figure]. All these graphs are obtained by direct numerical integration of the master equation (2.16), with $n_T = 0$.

E. Low-N behavior and spontaneous self-starting

The same mechanism explains why the $N=0$ solution can be quantum mechanically unstable. Even though expression (4.22) cannot be applied in this case, this can be explicitly verified again by direct numerical integration of (2.16). In Fig. 9, we plot the average number of photons as a function of time, for the case in which no triggering field is initially present in the cavity. For $\phi_{\rm int} = 3\pi/2$ and $N_{\rm ex} = 30$, the passage time is actually very small (of the order of a few $t_{\rm cav}$) already for $\sigma = 0$ and $n_T = 0$. As σ and n_T increase, this time becomes even smaller (Fig. 9 illustrates the dependence with n_T). This implies that, at least for not very large values of $N_{\rm ex}$, a triggering field is actually not necessary in order to start the maser oscillation.

The behavior of the starting time as a function of $\phi_{\rm int}$ is shown in Fig. 10(a). We notice that, for $\phi_{\rm int} \simeq 5\pi/2$, the starting time suddenly decreases, becoming of the order of $t_{\rm cav}$. This happens because, for such high pumping rates, $n=0$ is not even a minimum of $V_M(n)$. This can be seen explicitly from (4.1) and (4.2). Setting $N=0$ in (4.1), one gets

$$\rho_{11} = \frac{N_{\rm ex}}{N_T+1} \rho_{00} \left[1 - \int_0^\infty dt_{\rm int} P(t_{\rm int}) \, |A(0,t_{\rm int})|^2 + \frac{N_T}{N_{\rm ex}} \right]. \quad (4.23)$$

The mininum of the effective potential $V_M(n)$ (or, equivalently, the maximum of the probability distribution) at $N=0$ will disappear when $\rho_{11} > \rho_{00}$. Imposing this condition on (4.23), we find that this happens when

$$R \left[1 - \int_0^\infty dt_{\rm int} P(t_{\rm int}) \, |A(0,t_{\rm int})|^2 \right] > 1/t_{\rm cav} . \quad (4.24)$$

This relation has a simple physical interpretation. The left-hand side is the rate of production of photons by spontaneous emission, while the right-hand side is the cavity loss rate. Equation (4.24) simply states that $\rho_{11} > \rho_{00}$ if the spontaneous emission rate at $N=0$ is larger than the loss rate. In this case, the potential barrier around $N=0$ disappears and this point becomes unstable (of course, before this situation is attained, the point $N=0$ is already metastable).

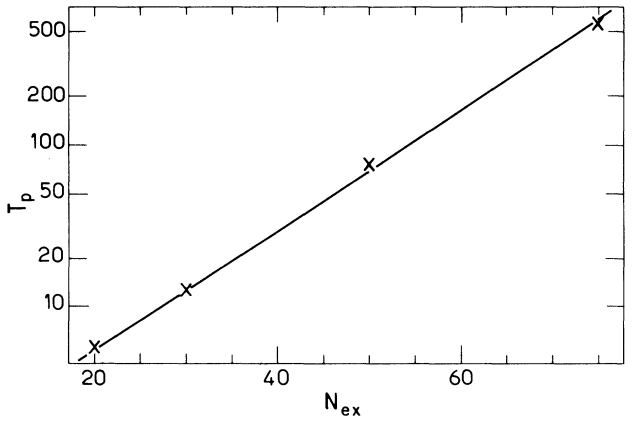

FIG. 8. Passage times as a function of $N_{\rm ex}$. Conditions are the same as in Fig. 7. T_p expressed in units of $t_{\rm cav}$.

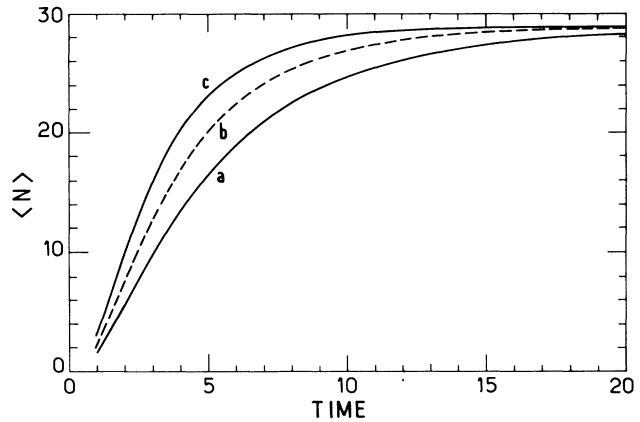

FIG. 9. Self-starting of the micromaser: $\langle N \rangle$ as a function of time (in units of $t_{\rm cav}$), when the cavity is initially in thermal equilibrium with *a*, $N_T = 0$; *b*, $N_T = 0.3$; *c*, $N_T = 0.7$. ($\phi_{\rm int} = 3\pi/2$ and $N_{\rm ex} = 30$ for the three curves.)

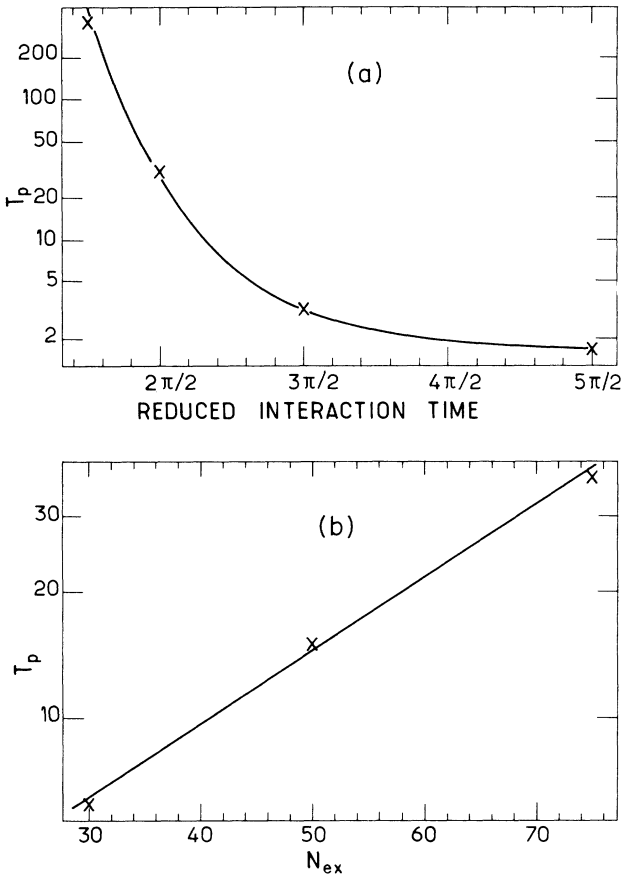

FIG. 10. Self-starting time as a function of (a) $\bar{\phi}_{int}$ for $N_{ex}=30$; (b) N_{ex} for $\bar{\phi}_{int}=3\pi/2$. We take $\sigma=0$ and $N_T=0$. T_p expressed in units of t_{cav}.

Taking (2.11) and (3.5) into account, we can write (4.24) in the form

$$(8N_{ex}/9)\int_0^\infty d\phi_{int}\tilde{P}(\phi_{int})\sin^2(3\phi_{int}/4N_{ex})>1\ . \quad (4.25)$$

For $\bar{\phi}_{int}/4N_{ex}\ll 1$, and for $\sigma\leq\bar{\phi}_{int}$, we can write approximately, from (4.25), that the condition for the potential barrier around $N=0$ to disappear is

$$\bar{\phi}_{int}>(2N_{ex}-\sigma^2)^{1/2}\ , \quad (4.26)$$

where we have used that $\bar{\phi}^2=(\bar{\phi})^2+\sigma^2$.

For $\sigma=0$ and $N_{ex}=30$, we find that the critical value of $\bar{\phi}_{int}$ is $4.9\pi/2$, consistent with the behavior shown in Fig. 10(a). The threshold lowers as σ increases, a consequence of the fact that the speed fluctuations add up to the spontaneous emission fluctuations in rendering the $N=0$ point unstable. In Fig. 10(b), we verify that, as long as $\bar{\phi}_{int}\leq 4.9\pi/2$, the escape time from $N=0$ grows exponentially with N_{ex}, thus extending to this region a result valid originally only for $N\gg 1$.

The above discussion shows that the condition for $N=0$ to be a local maximum of the probability distribution does not depend on the number of thermal photons. This is contrary to the semiclassical analysis, which predicts that this maximum should get displaced and should eventually disappear as n_T increases (cf. discussion in Sec. III). This discrepancy is due to the increase of the diffusion coefficient with N_T, smoothing out the potential around $N=0$. Furthermore, as N_T increases, the potential wells get flattened, and the passage time out of $N=0$ approaches indeed a value of the order of t_{cav}.

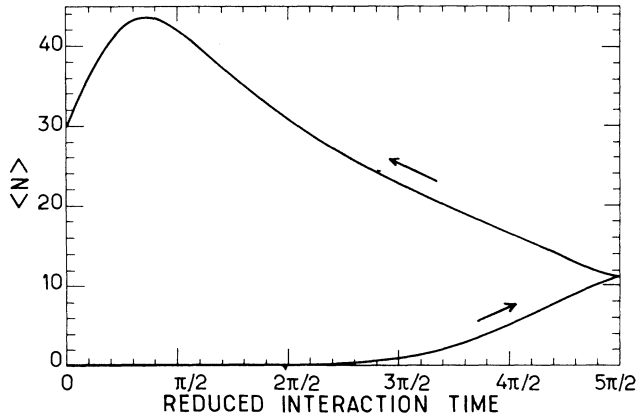

FIG. 11. Hysteresis cycle starting from $N=0$ for $N_{ex}=30$: $\langle N\rangle$ as a function of $\bar{\phi}_{int}$ when $\bar{\phi}_{int}$ changes linearly in time from 0 to $5\pi/2$ and then back to zero, in a time equal to $10t_{cav}$.

The above considerations allow us to predict a hysteresis cycle around $N=0$. Indeed, as $\bar{\phi}_{int}$ gets larger than the critical value (4.25), the system starts oscillating by itself in a time of the order of t_{cav}, going to the first minimum of the effective potential $V_M(n)$. Assume now that $\bar{\phi}_{int}$ is made to decrease past that critical value, in a scanning time much smaller than the passage time but much longer than t_{cav}. The average number of photons adiabatically follows the minimum of the evolving potential well, until this well finally disappears, at $\bar{\phi}_{int}\simeq 0.9\pi/2$, when $\langle N\rangle$ again goes to zero. The system stops oscillating therefore at a value of $\bar{\phi}_{int}$ smaller than the one for which it starts oscillating; we have thus a hysteresis cycle. We have verified this numerically, by direct integration of Eq. (2.16) with $N_T=0$, as shown in Fig. 11. The cycle duration is $10t_{cav}$. Note that in this figure $\langle N\rangle$ does not go back to zero. This is due to the fact that the end of the cycle, when the system is again below threshold, is swept in a time of the order of t_{cav}, so that the cavity field does not have time to decay completely.

Let us note that the metastability of the $N=0$ solution and the existence of hysteresis cycles in two-photon laser operation were already discussed in Ref. 9, which analyzed the evolution of a two-photon laser with thermal noise as a phase-transition phenomenon. This work was dealing with macroscopic lasers in which fluctuations alone are usually unable to start the oscillation if there is a potential well at $N=0$. It thus did not estimate the untriggered laser start-up time and focused instead on the behavior of triggered two-photon lasers. The theory in Ref. 9 was based on a Fokker-Planck equation different from the one presented here, which involved the field amplitude and not the photon-number distribution.

V. PHASE DIFFUSION AND SELF-INDUCED FREQUENCY PULLING

A. Fokker-Planck equation for nondiagonal elements

We apply now the method of Sec. IV to the off-diagonal elements of the density matrix. The elements $\rho_{N,N+1}$ determine the ensemble average of the electric field, according to

$$\langle E(t)\rangle = \mathcal{E}_0 \sum_N \rho_{N,N+1}(t)\sqrt{N+1}\exp(-i\omega t)+\text{c.c.} \ , \quad (5.1)$$

and therefore also the power spectrum and the maser linewidth. We analyze in this section the time-dependent behavior of $\rho_{N,N+1}$. In the Appendix C, we consider $\rho_{N,N+2}(t)$, which is important to discuss the squeezing properties of the field.

We set thus in (2.17) $M=N+1$, and introduce the normalized variable n, as before [Eq. (4.3)]. Setting

$$g(n,\tau)=\rho_{N,N+1}(t) \ , \quad (5.2)$$

where $\tau=Rt$, we get

$$\frac{d}{d\tau}g(n,\tau) = -g(n,\tau)\left[1-\int_0^\infty d\phi_{\text{int}}\tilde{P}(\phi_{\text{int}})\tilde{A}(n,\phi_{\text{int}})\tilde{A}^*(n+\delta,\phi_{\text{int}})\right]$$
$$+g(n-2\delta,\tau)\int_0^\infty d\phi_{\text{int}}\tilde{P}(\phi_{\text{int}})\tilde{B}(n,\phi_{\text{int}})\tilde{B}^*(n+\delta,\phi_{\text{int}})-[2n+\delta+4N_T(n+\delta)]g(n,\tau)$$
$$+2(N_T+1)\sqrt{(n+\delta)(n+2\delta)}g(n+\delta,\tau)+2N_T\sqrt{n(n+\delta)}g(n-\delta,\tau) \ . \quad (5.3)$$

Developing this equation in powers of δ, and keeping terms up to $O(\delta^2)$, we get

$$\frac{d}{d\tau}g(n,\tau) = -\mu(n)g(n,\tau)-\delta\frac{\partial}{\partial n}[b_1(n)g(n,\tau)]+\frac{\delta^2}{2}\frac{\partial^2}{\partial n^2}[a_2(n)g(n,\tau)]+O(\delta^2) \ , \quad (5.4)$$

where $a_2(n)$ is given by (4.11), and

$$\mu(n)=\delta^2\left[\int_0^\infty d\phi_{\text{int}}\tilde{P}(\phi_{\text{int}})\phi_{\text{int}}^2+\frac{1+2N_T}{4n}\right]+i\delta\left[\bar{\phi}_{\text{int}}-\frac{\delta}{2n}\int_0^\infty d\phi_{\text{int}}\tilde{P}(\phi_{\text{int}})\phi_{\text{int}}\left[1-\frac{\sin(2n\phi_{\text{int}})}{2n\phi_{\text{int}}}\right]\right] \ , \quad (5.5)$$

$$b_1(n)=2\left[\int_0^\infty d\phi_{\text{int}}\tilde{P}(\phi_{\text{int}})[(1-i\delta\phi_{\text{int}})\sin^2(n\phi_{\text{int}})+2\delta\phi_{\text{int}}\sin(2n\phi_{\text{int}})]-n+n_T-\delta/2\right] \ . \quad (5.6)$$

One should notice that $b_1(n)$ differs from $a_1(n)$, given by (4.10), by terms of order δ. Equation (5.4) differs from Eq. (4.9) also because of the presence of a term proportional to $g(n)$, in (5.4). We will show in the following that this term is very important, being associated with the decay of the ensemble average of the electric field and with the maser linewidth.

B. Phase diffusion and frequency pulling

Let $\bar{g}(n,\tau)$ be the solution of the equation

$$\frac{d}{d\tau}\bar{g}(n,\tau) = -\delta\frac{\partial}{\partial n}[b_1(n)\bar{g}(n,\tau)]$$
$$+\frac{\delta^2}{2}\frac{\partial^2}{\partial n^2}[a_2(n)\bar{g}(n,\tau)] \ . \quad (5.7)$$

This is a Fokker-Planck equation quite close to (4.9). Its stationary solution should be very close to $\rho^S(n)$. Furthermore, we will also have here two time scales, corresponding to the local and the global approach to equilibrium. If the initial distribution is close to one of the minima of the corresponding potential [which should be very close to the minima of $V_F(n)$], situated say at $n=n_L$, then, for times much smaller than the passage time, one can approximate n by n_L in $\mu(n)$. In this case, an approximate solution of (5.3) would be

$$g(n,\tau)\simeq\exp[-\mu(n_L)\tau]\bar{g}(n,\tau) \ . \quad (5.8)$$

For $t\gtrsim t_{\text{cav}}$, $\bar{g}(n,\tau)$ coincides with the local equilibrium distribution $g_L(n)$, and therefore $\mu(n_L)$ plays the role of a phase-diffusion constant, its real part being associated, as we can see from (5.1), to the exponential decay of the field. Of course, in order for this treatment to be consistent, it is necessary that the corresponding decay time be much larger than t_{cav}, while at the same time much smaller than the passage time. This will be shown below to be indeed the case, for sufficiently large N_{ex}.

Contrary to what happens in usual laser theory,[18] μ has an imaginary part, which corresponds to a frequency shift of the radiation in the cavity at resonance with the atomic transition. In real time units, one gets for the decay constant,

$$K=\frac{1}{4N_{\text{ex}}t_{\text{cav}}}\left[(\bar{\phi}_{\text{int}})^2+\sigma^2+\frac{1+2N_T}{4n_L}\right] \ , \quad (5.9)$$

while the frequency shift is given by

$$\Delta\omega\simeq\bar{\phi}_{\text{int}}/2t_{\text{cav}}=\Omega_{ei}^2N_{\text{ex}}\bar{t}_{\text{int}}/\Delta t_{\text{cav}} \ . \quad (5.10)$$

We can see therefore that the decay time of the off-diagonal matrix elements $\rho_{N,N+1}$ is of the order of $4N_{\text{ex}}t_{\text{cav}}$ (for $\bar{\phi}_{\text{int}}\sim n_L\sim 1$). For sufficiently large N_{ex},

this time will be indeed much larger than the local equilibrium time constant t_{cav} and much smaller than the global equilibrium time constant, which grows exponentially with N_{ex}. This means that $\rho_{N,N+1}(t)$ goes to zero before the long-time steady-state is attained, thus justifying the approximation $n \simeq n_L$ in $\mu(n)$. The associated linewidth, of the order of $(4N_{ex}t_{cav})^{-1}$, may be much smaller than the linewidth of the empty cavity.

In (5.9), the term

$$(1+2N_T)/16N_{ex}n_L t_{cav} = (1+2N_T)/8N_L t_{cav}$$

coincides precisely with the contribution from dissipation to the phase-diffusion rate in one-photon laser models.[18] The remaining contribution to (5.9) comes from the pumping, and it is also present, although not in the same form, in the usual laser models.[18]

The frequency shift, on the other hand, is quite characteristic of the two-photon micromaser, and can be interpreted as a self-induced frequency pulling, which occurs in spite of the fact that the atoms are initially in resonance with the cavity. This frequency pulling originates from a quadratic ac Stark shift between states $|e\rangle$ and $|f\rangle$ induced by the field in the cavity, via the intermediate state $|i\rangle$. According to Refs. 15 and 17, this shift is given by

$$\frac{\Omega_{ei}^2(N+2)}{\Delta} - \frac{\Omega_{ei}^2(N+1)}{\Delta} = \frac{\Omega_{ei}^2}{\Delta} , \tag{5.11}$$

so that the atom, after entering the cavity, is no longer in resonance with the field. As in the frequency-pulling effect,[18] the refractive index of the atomic medium produces then a shift in the frequency of the field inside the cavity. For one-photon masers, this Stark shift is much smaller (in fact, it is absent in two-level atom models), so frequency pulling is usually negligible when the atoms are resonant with the cavity. In the two-photon maser, the shift $\Delta\omega$ can be much larger than the cavity width $1/t_{cav}$, when $\bar{\phi}_{int} \gg 1$ [see Eq. (5.10)].

We display in Fig. 12 the time-dependent behavior of $\mathrm{Re}[\rho_{N,N-1}(t)]$, for $N=29$ as calculated numerically from Eq. (2.16), with n_T set equal to zero for simplicity. We take $\phi_{int}=3\pi/2$, and assume that the initial state is a coherent one, with $\langle N\rangle=29$. Both the decay constant and the frequency of the oscillations agree precisely with the values given by (5.9) and (5.10). One should notice that Eq. (2.16) yields $\rho(t)$ in interaction representation, so that these oscillations actually represent the beating between the field and the cavity frequencies [cf. Eq. (5.1)].

We show in Appendix B that the δ-expansion method offers a natural way to find the phase-diffusion constant in the usual laser theory, and we apply it also to find the phase-diffusion constant in the one-photon micromaser.

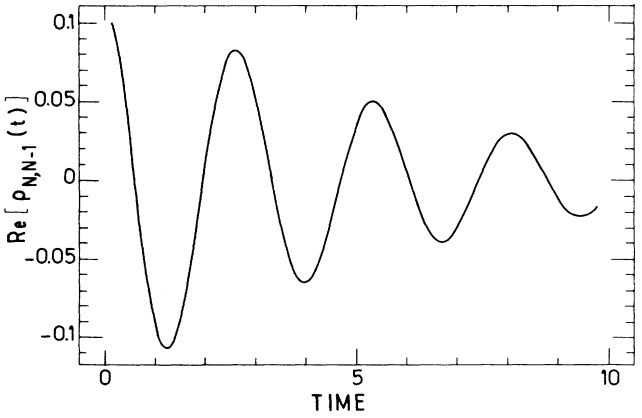

FIG. 12. Time-dependent behavior of $\mathrm{Re}[\rho_{N,N-1}(t)]$ for $N=29$. The initial state is a coherent one with $\langle N\rangle=29$, which corresponds to the absolute minimum of V_M ($\phi_{int}=3\pi/2$). The decay time coincides with the phase-diffusion time found in the text, while the oscillation frequency is given by the self-induced frequency shift. $N_{ex}=30$, $\sigma=0$, $n_T=0$. Time expressed in units of t_{cav}.

VI. SUB-POISSONIAN STATISTICS

It has been shown that the field inside the cavity in a one-photon micromaser presents, under certain conditions, a sub-Poissonian statistics.[13] On the other hand, it has been pointed out that the field emitted by two-photon lasers might present interesting statistical properties, and that these devices could be used to generate "squeezed" states of light.[5,6] One should therefore expect to find these properties for a two-photon micromaser.

The normalized variance of the field inside the cavity,

$$V = (\langle N^2\rangle - \langle N\rangle^2)^{1/2}/\langle N\rangle^{1/2} ,$$

as a function of ϕ_{int}, is shown in Fig. 13. Again, this variance was numerically calculated from the steady-state distributions resulting from (4.1) and (4.2). The field is seen to exhibit a sub-Poissonian statistics from $\phi_{int} \simeq 1.5\pi/2$ to $\phi_{int} \simeq 6.5\pi/2$ (we take $\sigma=0$ and $N_T=0$). As $\phi_{int} \to \infty$, the variance tends to a limiting value, which coincides with the variance of the limiting distribution (4.20).

The large peak in Fig. 13 corresponds to the situation

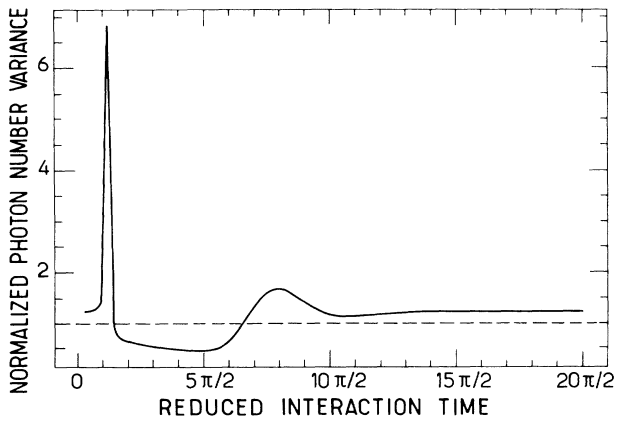

FIG. 13. Evidence of sub-Poissonian statistics: normalized photon-number variance of the field inside the cavity as a function of ϕ_{int} ($\sigma=0$, $n_T=0$, $N_{ex}=30$).

depicted in Fig. 3(b), in which the minimum of the potential outside the origin has about the same height as the one at the origin. This implies that the photon-number distribution displays two peaks of approximately equal height, thus yielding a large variance. A similar argument holds for the peak around $\phi_{\rm int}=8\pi/2$, in Fig. 13; the two minima displayed in Fig. 3(c) have comparable heights, for this value of $\phi_{\rm int}$.

In Appendix C we discuss the fluctuation properties of the field. For values of $N_{\rm ex}$ up to 75, only a very small transient squeezing is found. In fact, squeezing is strongly affected by phase diffusion, so we should expect it to become more important for larger values of $N_{\rm ex}$, when phase-diffusion times get longer. A more complete treatment will be presented elsewhere.

VII. CONCLUSION

Quantum effects may have a substantial influence on the behavior of the two-photon micromaser. They are specially important when the pumping rate is not very high (low $N_{\rm ex}$). They make unstable the $N=0$ photon state, which according to semiclassical theory is always stable, and they also change the effective threshold for laser oscillation.

The formalism we have developed is particularly useful for the calculation of these effects. It leads to a Fokker-Planck equation for the photon-number distribution, and it allows the calculation of phase-diffusion effects for the micromaser. It represents also a very natural approach to this problem in usual laser theory. For the specific case of the two-photon micromaser, the diffusion coefficient is found to be complex, its imaginary part corresponding to a frequency shift of the field inside the cavity.

One should stress that all the predictions in this paper concern the field *inside* the cavity. The statistical properties of the field can be substantially altered by the transmission to the region outside the cavity.[24–26]

The question arises then as to how these properties of the field could be experimentally tested. They could in principle be probed by an extra atomic beam, sufficiently weak so as to have a negligible effect on the field which is being measured. The upper-state population of the outgoing atoms is given by the atomic reduced density matrix, which is obtained from (2.10),

$$\rho_{ee}(t_i+\Delta t)=\sum_N \rho_{NN}(t_i)\,|\,A(N,\Delta t)\,|^2\ , \tag{7.1}$$

where $\rho_{ee}(t_i+\Delta t)$ is the upper-state population of the atoms which have entered the cavity at time t_i and interacted with it during a time Δt. Study of $\rho_{ee}(t_i+\Delta t)$ as a function of Δt yields therefore information on $\rho_{NN}(t_i)$. On the other hand, the atomic coherence yields information on $\rho_{N,N-2}$:

$$\rho_{ef}(t_i+\Delta t)=\sum_N \rho_{N,N-2}(t_i)\,A(N,\Delta t)B^*(N,\Delta t)\ , \tag{7.2}$$

and therefore on the squeezing properties of the field.

The above results evidently concern quantum averages over an ensemble of identically prepared systems. They are not related, therefore, to the more current experimental procedure of continuously monitoring the system. In particular, the observation of multistability and tunneling in a single realization of the experiment cannot be discussed directly in terms of those ensemble averages; the dynamical behavior of a continuously monitored system evolving from an equilibrium state to another remains an open question, somewhat related to the "quantum jump" problem.[27–29] This subject is, however, outside the scope of this paper, and will be addressed elsewhere.

Note added in proof. Successful operation of the two-photon continuous-wave maser described here has been achieved in our laboratory after this article was submitted. The device oscillates on the $40S\rightarrow 39S$ two-photon transition of Rb.[30]

ACKNOWLEDGMENTS

We would like to thank the members of "Groupement de Recherches Coordonnées 70 [Centre National de la Recherche Scientifique (CNRS)]: Expérimentation Numérique" for making their computers available to us. One of us (L.D.) wishes to acknowledge the hospitality of Ecole Normale Supérieure and the financial support of CNRS and Coordenaçâo de Aperfeiçoamento de Pessoal do Ensino Superior.

APPENDIX A: DERIVATION OF A SCULLY-LAMB EQUATION OF MOTION FOR THE MICROMASER

We discuss in this appendix the assumptions which lead to Eq. (2.13) for the reduced density matrix ρ of the field inside the micromaser cavity.

As in the Scully-Lamb approach to laser theory, we assume that dissipation can be neglected when calculating the change of ρ due to the interaction with a single atom. This should be true if the interaction time $t_{\rm int}$ of each atom with the field inside the cavity is much smaller than the cavity damping time $t_{\rm cav}$. In this approximation, the contribution from the single atom and the field loss reservoir are considered to be independent. This is actually quite apparent in Eq. (2.13).

We suppose yet that one atom at most interacts with the cavity field at a time. Let t_i be the time when the ith atom enters the cavity. We write then

$$\rho(t_{i+1})=e^{L\Delta t_i}F(t_{\rm int})\rho(t_i)\ , \tag{A1}$$

where the operator $F(t_{\rm int})$ describes the change of $\rho(t_i)$ due to the interaction with a single atom and the exponential describes field relaxation during $\Delta t_i=t_{i+1}-t_i$.

We do not assume here that the operator $F(t_{\rm int})$ is close to unity [in this case, it is easy to show that (2.13) follows from (A1) without any further assumption, by setting $F=1+\delta F$, $e^{L\Delta t_i}\simeq 1+L\Delta t_i$, and neglecting the product $L\delta F\Delta t_i$]. This is not allowed in our case, since each atom develops one or more Rabi oscillations while transiting through the cavity.

We assume instead, as in Ref. 13, that the incoming atoms obey a Poisson distribution, which implies an exponential distribution for the time intervals between two successive atoms:

$$P(\Delta t_i)=Re^{-R\Delta t_i}\ , \tag{A2}$$

R^{-1} being the average time interval (t_{at}). The density operator is now a function of the random variables Δt_i, assumed to be statistically independent. The statistical average is given by

$$\bar{\rho}(t_{i+1}) = \int_0^\infty d\Delta t_i R e^{-R\Delta t_i} e^{L\Delta t_i} F(t_{int})\bar{\rho}(t_i) = \frac{1}{1-\frac{L}{R}} F(t_{int})\bar{\rho}(t_i) \ . \quad \text{(A3)}$$

In (A3) we have decorrelated the average over the product $e^{L\Delta t_i} F(t_{int})\rho(t_i)$, since $\rho(t_i)$ does not depend on Δt_i (it depends only on the previous time intervals).[13] We get then, from this expression,

$$R[\bar{\rho}(t_{i+1})-\bar{\rho}(t_i)] = L\bar{\rho}(t_{i+1}) + R[F(t_{int})\bar{\rho}(t_i)-\bar{\rho}(t_i)] \ . \quad \text{(A4)}$$

Since $\Delta t_i \ll t_{cav}$, one can replace the left-hand side of (A4) by $\dot{\rho}$, and $L\bar{\rho}(t_{i+1})$ by $L\bar{\rho}(t_i)$. This amounts to assuming that the *statistically averaged* $\bar{\rho}$ does not change much between t_i and t_{i+1} [before this average is taken, the operator $\rho(t)$ may present large fluctuations, due to the fact that $F(t_{int})$ is not close to unity; this is made evident for instance by Fig. 8 of Ref. 15]. One gets thus the rate equation (2.13). For the sake of notational simplicity we suppress in the text the bar over ρ.

We see therefore that, when $F(t_{int})$ is not close to unity, a Poissonian atomic distribution is implicit when writing (2.13). Indeed, using arguments similar to those in Ref. 13, one can show that the diffusion coefficient $a_2(n)$, given by (4.11), corresponds to a Poissonian distribution of the incoming atoms.

APPENDIX B: PHASE DIFFUSION IN THE SCULLY-LAMB MODEL OF THE ONE-PHOTON LASER

We show here that the δ-expansion method provides a very natural way of getting the phase-diffusion constant in usual laser theory.

We start from the Scully-Lamb equation of motion for the off-diagonal matrix elements of the laser field reduced density operator [Eq. (16) of Chap. 17 of Ref. 18]:

$$\dot{\rho}_{N,N+1} = -\frac{1}{2}\frac{(2N+3)A+B/4}{1+B(2N+3)/2A+(B/4A)^2}\rho_{N,N+1} + \frac{A[N(N+1)]^{1/2}}{1+B(2N+1)/2A+(B/4A)^2}\rho_{N-1,N} - \frac{C}{2}(2N+1)\rho_{N,N+1} + C\sqrt{(N+1)(N+2)}\rho_{N+1,N+2} \ , \quad \text{(B1)}$$

where

$$A = 2r_a(g/\gamma)^2 \ , \quad \text{(B2)}$$

$$B = 8r_a(g/\gamma)^4 \ , \quad \text{(B3)}$$

$$C = \omega/Q = t_{cav}^{-1} \ . \quad \text{(B4)}$$

r_a is the atomic pumping rate into the excited state, g is the atom-field-coupling constant, and γ^{-1} is the atomic lifetime. Evidently, r_a corresponds to our pumping rate R and γ^{-1} is related to t_{int}. We have in particular $r_a = N_{ex}/t_{cav}$.

We define now

$$\Theta = g(2N_{ex})^{1/2}/\gamma \ , \quad \text{(B5)}$$

so that

$$A = \Theta^2/t_{cav}, \quad B = 2\Theta^4/N_{ex}t_{cav} \ . \quad \text{(B6)}$$

The threshold for oscillation is given by the condition[18] $A = C$, and therefore corresponds to $\Theta = 1$.

We define also

$$n = N/N_{ex}, \quad \delta = 1/N_{ex}, \quad g(n,\tau) = \rho_{N,N+1}(t) \ , \quad \text{(B7)}$$

where τ is the dimensionless time

$$\tau = r_a t \ . \quad \text{(B8)}$$

Equation (B1) becomes then

$$\frac{d}{d\tau}g(n,\tau) = -\frac{1}{2}\frac{\Theta^2(2n+3\delta)+\Theta^4\delta^2/2}{1+\Theta^2(2n+3\delta)+\Theta^4\delta^2/4}g(n,\tau) + \frac{\Theta^2\sqrt{n(n+\delta)}}{1+\Theta^2(2n+\delta)+\Theta^4\delta^2/4}g(n-\delta,\tau) - \left[n+\frac{\delta}{2}\right]g(n,\tau) + \sqrt{(n+\delta)(n+2\delta)}g(n+\delta,\tau) \ . \quad \text{(B9)}$$

Developing now this expression in powers of δ, we get

$$\frac{d}{d\tau}g(n,\tau) = -\mu(n)g(n,\tau) - \delta\frac{\partial}{\partial n}[f_1(n)g(n,\tau)] + \frac{\delta^2}{2}\frac{\partial^2}{\partial n^2}[f_2(n)g(n,\tau)] + O(\delta^3) \ , \quad \text{(B10)}$$

where

$$\mu(n) = \frac{\delta^2}{8n}(1+\Theta^2) \ , \quad \text{(B11)}$$

$$f_1(n) = \frac{\Theta^2}{1+2\Theta^2 n}\left[n+\frac{3\delta/2}{1+2\Theta^2 n}\right] - n - \frac{\delta}{2} \ , \quad \text{(B12)}$$

$$f_2(n) = \frac{\Theta^2 n}{1+2\Theta^2 n} + n \ . \quad \text{(B13)}$$

As in the two-photon maser case (see Sec. V), $f_1(n)$ and $f_2(n)$ are, within terms of the order of δ, identical to the drift and diffusion coefficients of the Fokker-Planck equation for the diagonal photon-number distribution $\rho(n,\tau)$. If $\mu(n)$ were equal to zero, $g(n,\tau)$ would thus evolve rapidly into a steady state approximately equal to the steady-state photon-number distribution $\rho_S(n)$. There is only one potential minimum around

$$n_S = \frac{1}{2}\left[1-\frac{1}{\Theta^2}\right] \quad \text{(B14)}$$

for the Scully-Lamb model discussed here and the steady

state is reached within a time of order t_{cav}. If the laser is well above threshold, $\rho_S(n)$ is well peaked around n_S. Taking now into account the term proportional to $\mu(n)$, we can approximate the solution of (B10) by the adiabatic expression

$$g(n,\tau)\simeq\rho_S(n)e^{-\mu(n_S)\tau} . \tag{B15}$$

The field expectation value thus decays with a rate which can be identified with the phase-diffusion coefficient and which, in real time units, is

$$\mu=r_a\mu(n_S)=(1+\Theta^2)/8N_S t_{cav} , \tag{B16}$$

where $N_S=n_S N_{ex}$ is the average value of N in steady state. The constant μ, given by Eq. (B16), is indeed much smaller than t_{cav}^{-1}, which validates the adiabatic approximation made in writing Eq. (B15).

Expression (B15) corresponds precisely to the Scully-Lamb ansatz,[18] to which we arrive, in the present formalism, in a very natural way. The phase-diffusion constant (B16) coincides with the one found by Scully and Lamb,[18] in spite of the fact that, in our treatment, no expansion of the equation (B1) in powers of B/A has been made.

In the usual Scully-Lamb model, the atom-cavity interaction time is averaged over an exponential distribution.[18] It is possible to consider instead a fixed interaction time t_{int}, as is usually done in the context of micromaser studies.[13,31] In this case, multistable operation of the system becomes possible, exactly as in the two-photon maser situation discussed in this paper. The method of this appendix can again be applied in order to obtain the phase-diffusion coefficient in this case. We start from the corresponding equation of motion for the reduced density operator of the field:[13,31]

$$\begin{aligned}\frac{d}{d\tau}g(n,\tau)=&g(n,\tau)[\cos(\phi\sqrt{n+\delta})\cos(\phi\sqrt{n+2\delta})-1]\\&+g(n-\delta,\tau)\sin(\phi\sqrt{n})\sin(\phi\sqrt{n+\delta})\\&-\tfrac{1}{2}(2n+\delta)g(n,\tau)\\&+\sqrt{(n+\delta)(n+2\delta)}\,g(n+\delta,\tau) ,\end{aligned} \tag{B17}$$

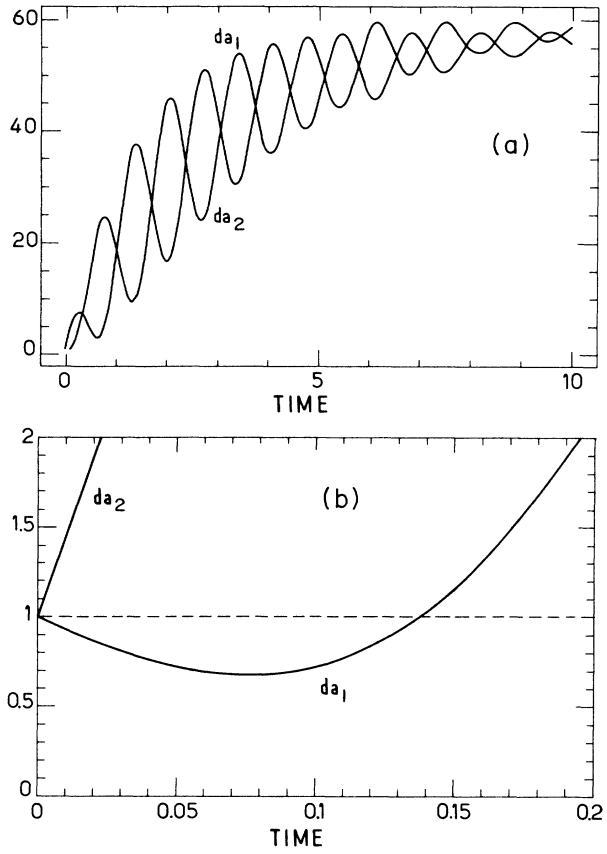

FIG. 14. Evolution of the quadrature components variances of the field inside the cavity. The decay time is twice the phase-diffusion time, while the oscillation frequency is twice the frequency shift. (a) Same conditions as in Fig. 12 ($N_{ex}=30$); (b) evidence of squeezing for $N_{ex}=75$, other conditions being the same as in (a). Squeezing is strongly affected by phase diffusion for this value of N_{ex}. Times are expressed in units of t_{cav}.

where we have used the definitions (B7) and (B8), and we have further defined

$$\phi=(N_{ex})^{1/2}gt_{int} . \tag{B18}$$

Developing (B17) in powers of δ, we get

$$\begin{aligned}\frac{d}{d\tau}g(n,\tau)=&-\frac{\delta^2}{8n}(1+\phi^2)g(n,\tau)-\delta\frac{\partial}{\partial n}\left[g(n,\tau)\left[\sin^2(\phi\sqrt{n})-\frac{\phi\delta}{4\sqrt{n}}\sin(2\phi\sqrt{n})-n-\frac{\delta}{2}\right]\right]\\&+\frac{\delta^2}{2}\frac{\partial^2}{\partial n^2}\{g(n,\tau)[\sin^2(\phi\sqrt{n})+n]\}+O(\delta^3) .\end{aligned} \tag{B19}$$

From this equation, we get the phase-diffusion constant

$$\mu=(1+\phi^2)/8N_L t_{cav} ,$$

where N_L is the number of photons associated with the local maximum of the steady-state distribution which is closest to the initial average photon number (assuming that the initial distribution is sufficiently sharp—cf. discussion in Sec. V B). This result makes it clear that the frequency shift found in Sec. V B is indeed a peculiarity of two-photon micromasers.

APPENDIX C: FLUCTUATIONS IN THE TWO-PHOTON MICROMASER

In order to discuss the fluctuation properties of the field, let us consider the quadrature components,

$$a_1 = a + a^\dagger, \quad a_2 = (a - a^\dagger)/i \ . \tag{C1}$$

Let da_1 and da_2 be the variances of a_1 and a_2, respectively. Squeezing will occur if either da_1 or da_2 gets smaller than 1.[21–23]

From

$$da_1 = 2\mathrm{Re}\langle a^2 \rangle + 1 + 2\langle a^\dagger a \rangle - 4\mathrm{Re}^2\langle a \rangle \ , \tag{C2}$$

$$da_2 = -2\mathrm{Re}\langle a^2 \rangle + 1 + 2\langle a^\dagger a \rangle - 4\mathrm{Im}^2\langle a \rangle \ , \tag{C3}$$

it is clear that these variances depend on ρ_{NN}, $\rho_{N,N+1}$, and $\rho_{N,N+2}$. Since the off-diagonal elements of the density matrix go to zero as $t \to \infty$, it follows that in this limit da_1 and da_2 go to $1+2\langle N \rangle$, and therefore the steady state presents no squeezing.

Squeezing could occur, however, after the establishment of local equilibrium, but before phase diffusion takes place, that is, for times larger than t_{cav} but smaller than K^{-1} given by (5.9).

A Fokker-Planck type equation for $\rho_{N,N+2}$ can be calculated in the same way as above for $\rho_{N,N+1}$. Let $h(n,\tau) = \rho_{N,N+2}(t)$, with n defined by (4.3) and $\tau = Rt$. We find then, setting for simplicity $n_T = 0$ and $\sigma = 0$,

$$\begin{aligned}\frac{d}{d\tau}h(n,\tau) = &-h(n,\tau)\left\{4\delta^2\left[\phi_{\mathrm{int}} + \frac{1}{4n}\right] + 2i\delta\phi_{\mathrm{int}}\left[1 - \frac{\delta}{2n}\left[1 - \frac{\sin(2n\phi_{\mathrm{int}})}{2n\phi_{\mathrm{int}}}\right]\right]\right\} \\ &+ \delta\frac{\partial}{\partial n}\left(h(n,\tau)\{\cos(2n\phi_{\mathrm{int}}) - 5\delta\phi_{\mathrm{int}}\sin(2n\phi_{\mathrm{int}}) - 1 + 2n + 2\delta - 2i\delta\phi_{\mathrm{int}}[\cos(2n\phi_{\mathrm{int}}) - 5\delta\phi_{\mathrm{int}}\sin(2n\phi_{\mathrm{int}})]\}\right) \\ &+ \delta^2\frac{\partial^2}{\partial n^2}\{h(n,\tau)[1 - \cos(2n\phi_{\mathrm{int}}) + n]\} + O(\delta^3) \ .\end{aligned} \tag{C4}$$

It follows from this expression that the decay time for $\rho_{N,N+2}$ is four times smaller than the decay time for $\rho_{N,N+1}$, while the oscillation frequency of $\rho_{N,N+2}$ is twice the frequency of $\rho_{N,N+1}$. This implies that the term $\mathrm{Re}\langle a^2 \rangle$ in (C2) and (C3), which depends on $\rho_{N,N+2}$, will decay two times faster than the terms $\mathrm{Re}^2\langle a \rangle$ and $\mathrm{Im}^2\langle a \rangle$, which involve $\rho_{N,N+1}$. It is clear also that da_1 and da_2 will oscillate with a frequency equal to twice the frequency shift found in Sec. V. These predictions are precisely verified by the numerical calculation, starting from the master equation (2.16), of da_1 and da_2. The result is exhibited in Fig. 14, which also displays the occurrence of a very small transient squeezing of the field.

*Permanent address: Departamento de Fisica, Pontificia Universidade Catolica, 22453 Rio de Janeiro, Brazil.
†Also at Yale University, New Haven, CT 06520.

[1] P. P. Sorokin and N. Braslau, IBM J. Res. Dev. **8**, 177 (1964).
[2] A. M. Prokhorov, Science, **149**, 828 (1965).
[3] V. S. Letokhov, Pis'ma Zh. Eksp. Teor. Fiz. **7**, 284 (1968) [JETP Lett. **7**, 221 (1968)].
[4] K. J. McNeil and D. F. Walls, J. Phys. A **8**, 104, 111 (1975).
[5] H. P. Yuen, Phys. Lett. **51A**, 1 (1975).
[6] H. P. Yuen, Phys. Rev A **13**, 226 (1976).
[7] L. M. Narducci, W. W. Eidson, P. Furcinitti, and D. C. Eteson, Phys. Rev. A **16**, 1665 (1977).
[8] T. Hoshimiya, A. Yamagishi, N. Tanno, and H. Inaba, Jpn. J. Appl. Phys. **17**, 2177 (1978); N. Nayak, B. K. Mohanty, Phys. Rev. A **19**, 1204 (1979).
[9] Z. C. Wang and H. Haken, Z. Phys. B **55**, 361 (1984); **56**, 77 (1984); **56**, 83 (1984).
[10] B. Nikolaus, D. Z. Zhang, and P. E. Toschek, Phys. Rev. Lett. **47**, 171 (1981); M. M. T. Loy, *ibid.* **41**, 473 (1978); H. Schlemmer, D. Frölich, and H. Welling, Opt. Commun. **32**, 141 (1980).
[11] P. Goy, J. M. Raimond, M. Gross, and S. Haroche, Phys. Rev. Lett. **50**, 1903 (1983).
[12] D. Meschede, H. Walther, and G. Müller, Phys. Rev. Lett. **54**, 551 (1985).
[13] P. Filipowicz, J. Javanainen, and P. Meystre, Phys. Rev. A **34**, 3077 (1986).
[14] P. Filipowicz, J. Javanainen, and P. Meystre, Opt. Commun. **58**, 327 (1986).
[15] M. Brune, J. M. Raimond, and S. Haroche, Phys. Rev. A **35**, 154 (1987).
[16] D. Grischkowsky, M. M. T. Loy, and P. F. Liao, Phys. Rev. A **12**, 2514 (1975).
[17] H. I. Yoo and J. H. Eberly, Phys. Rep. **118**, 239 (1985).
[18] M. Sargent III, M. O. Scully, and W. E. Lamb, *Laser Physics* (Addison-Wesley, Reading, Mass., 1974).
[19] N. G. Van Kampen, *Stochastic Processes in Physics and Chemistry* (North-Holland, Amsterdam, 1981).
[20] R. J. Glauber, in *Optical Coherence and Photon Statistics*, Proceedings of the Les Houches Summer School, edited by C. de Witt, A. Blandin, and C. Cohen-Tannoudji (Gordon and Breach, New York, 1965).

[21]D. F. Walls, Nature (London) **306**, 141 (1983), and references therein.
[22]A. Heidmann, J. M. Raimond, and S. Reynaud, Phys. Rev. Lett. **54**, 326 (1985).
[23]A. Heidmann, J. M. Raimond, S. Reynaud, and N. Zagury, Opt. Commun. **54**, 189 (1985).
[24]B. Yurke, Phys. Rev. A **29**, 408 (1984).
[25]M. J. Collet and C. W. Gardiner, Phys. Rev. A **31**, 3761 (1985).
[26]M. J. Collet and D. F. Walls, Phys. Rev. A **32**, 2887 (1985).
[27]R. J. Cook and H. J. Kimble, Phys. Rev. Lett. **54**, 1023 (1985).
[28]J. Javanainen, Phys. Rev. A **33**, 2121 (1986).
[29]C. Cohen-Tannoudji and J. Dalibard, Eur. Phys. Lett. **1**, 441 (1986).
[30]M. Brune, J. M. Raimond, P. Goy, L. Davidovich, and S. Haroche (unpublished).
[31]J. Krause, M. O. Scully, and H. Walther, Phys. Rev. A **34**, 2032 (1986).